# Electromagnetic probes of nuclear structure: Sum rules, $y$ scaling, and final state interactions

L. S. Celenza and C. M. Shakin
*Department of Physics and Center for Nuclear Theory, Brooklyn College of the City University of New York, Brooklyn, New York 11210*

W. Koepf
*Physikdepartment der Technischen Universitaet Muenchen, D-8046 Garching, Federal Republic of Germany*
(Received 11 May 1990)

We study the response to an electromagnetic probe of a simple system of two scalar particles ("nucleons") bound to form a scalar "deuteron." The use of a covariant separable interaction allows for an elementary solution of the Bethe-Salpeter equation for both the bound state and for the scattering amplitude. Knowledge of the scattering amplitude allows for an exact treatment of the final state interactions within the limitations of the model. We present results for structure functions and sum rules for a large range of momentum transfer. We also present a systematic study of $y$ scaling and discuss the role of the final state interactions in our model. As noted by other authors, we see that $y$ scaling is well satisfied at the quasielastic peak; however, significant deviations from such scaling behavior are seen in our results as one moves away from the quasielastic peak to the region of large, negative $y$. We also discuss the influence of final state interactions in modifying sum rules which are well satisfied in the plane wave Born approximation at all $Q^2$.

## I. INTRODUCTION

The study of nuclear structure using electromagnetic probes is a well explored area, and extensive further experimental studies will be performed at the Continuous Electron Beam Accelerator Facility (CEBAF) which is presently under construction. In the past decade many experiments have been performed which have led us to question whether we have a good understanding of nuclear structure or whether the reaction theory used in interpreting experiments is sufficiently well developed such that definitive conclusions may be drawn from the experimental data. Of the various experiments performed we may concentrate our discussion on the phenomenon of "$y$ scaling." Following the original theoretical work of West[1] and subsequent experimental studies[2] there have been a large number of theoretical investigations[3-10] dealing with the interpretation of the data. A significant body of the theoretical work has dealt with problems associated with final state interactions[4,6] which may interfere with the extraction of nucleon momentum distributions from the $y$-scaling data. It is not our goal to review that body of work. Rather we are interested in describing a very simple relativistic model which can be solved completely. Our aim is to study the electromagnetic response of a simple system so that we can understand the approach to scaling behavior and how such behavior is affected by final state interactions. (We are able to discuss both $x$ scaling and $y$ scaling; however, it is only $y$ scaling which is relevant to nuclear structure physics.) We are also able to discuss the "Coulomb sum rule" for our problem and to see how final state interactions affect that sum rule.

In this work we use a separable covariant interaction to solve the two-body problem. The utility of such approximations may be seen in the work of Tjon and collaborators[11-13] which provided some motivation for the investigation reported here.

The organization of our work is as follows. In Sec. II we describe the model and in Sec. III we discuss the calculation of the "deuteron form factor." Section IV provides a discussion of the hadronic tensor in the plane wave impulse approximation. In Sec. V we discuss $x$ scaling and sum rules. In Sec. VI we return to a discussion of the hadronic tensor and include the effects of final state interactions in our calculation. Section VII is devoted to a discussion of $y$ scaling, while in Sec. VIII we discuss the numerical results we have obtained. Section IX contains some further discussion and conclusions.

## II. THE MODEL

In order to understand various properties of the electromagnetic response without obscuring our discussion with complex algebra, we will neglect the spin of the particles in the formulation of the model, i.e., we consider a "scalar deuteron" composed of "scalar nucleons." Our starting point is the Bethe-Salpeter equation,[14] a linear integral equation, which provides a covariant description of the scattering and of the bound state of two particles:[15]

$$T(p',p;P)=V(p',p;P)+i\int\frac{d^4k}{(2\pi)^4}V(p',k;P)G(k)\times G(P-k)T(k,p;P)\ . \tag{2.1}$$

This equation is depicted in Fig. 1. Here $T$ is the off-shell scattering amplitude, $V$ stands for the set of all two-particle irreducible graphs,[11] and $G(k)$ is the Green's

 

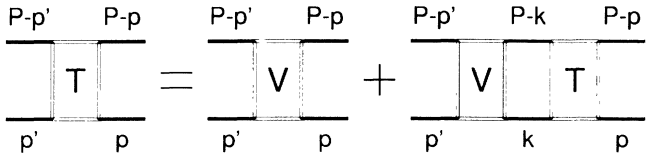


FIG. 1. The Bethe-Salpeter equation in momentum space. $T$ is the off-shell scattering amplitude and $V$ stands for the set of all two-particle irreducible graphs.

function for a scalar particle with momentum $k$ and mass $m$,

$$G(k)=\frac{1}{k^2-m^2+i\varepsilon} . \tag{2.2}$$

We make a rank-one separable Ansatz for the interaction $V$:

$$V(p',p;P)=\lambda g(p';P)g(p;P) . \tag{2.3}$$

The formalism we use is covariant. It may be seen that the interaction defined in Eq. (2.3) is of $S$ wave character in the center-of-mass frame. The integral equation [Eq. (2.1)] can be solved in closed form, yielding

$$T(p',p;P)=\frac{\lambda g(p';P)g(p;P)}{D(s)} . \tag{2.4}$$

The denominator function, $D(s)$, is a function of only the invariant mass $s=P^2$,

$$D(s)=1-i\lambda\int\frac{d^4k}{(2\pi)^4}g(k;P)G(k)G(P-k)g(k;P) . \tag{2.5}$$

The existence of a two-particle bound state corresponds to a pole in the $T$ matrix in the variable $s$,

$$D(s=M^2)=0 . \tag{2.6}$$

Here $M$ denotes the "deuteron" mass. The vertex function of this bound state is

$$\Gamma(k;P)=Ng(k;P) , \tag{2.7}$$

which we will need for the calculation of the matrix elements of the electromagnetic current. The normalization factor of the Bethe-Salpeter wave function, $N$, is calculated using charge conservation, i.e., $F_0(Q^2=0)=1$, where $F_\mu(Q^2)$ is the matrix element of the electromagnetic current, which will be calculated in the following section.

To further simplify the problem we choose the covariant form factor, $g(k;P)$, to depend only on a single variable $k_c^2$. We put $g(k;P)=g(k_c^2)$, with

$$k_c^2=\frac{[P\cdot(P/2-k)]^2-P^2(P/2-k)^2}{P^2} . \tag{2.8}$$

The variable $k_c$ is the relative momentum in the center-of-mass frame, i.e., it reduces to $|\mathbf{k}|$ for $P=(M,\mathbf{0})$. (For example, this variable was used previously in an application of the Bethe-Salpeter equation in the study of the bound state of two scalar particles.[16]) We choose a specific shape for the form factor $g(k_c^2)$,

$$g(k_c^2)=\left[\frac{32\pi}{m}\right]^{1/2}(k_c^2+m^2)^{1/4}\frac{\Lambda^2}{k_c^2+\Lambda^2} . \tag{2.9}$$

This is a covariant generalization[13] of a Yamaguchi-type expression. The factor $1/(k_c^2+\Lambda^2)$ reduces to $1/(|\mathbf{k}|^2+\Lambda^2)$ in the center-of-mass frame, and this term is the Fourier transform of a Yukawa potential local in time:

$$\frac{1}{|\mathbf{k}|^2+\Lambda^2}=\int d^4x\, e^{ik\cdot x}\delta(t)\frac{e^{-\Lambda r}}{4\pi r} . \tag{2.10}$$

The second factor in $g(k_c^2)$, taken to the power $\frac{1}{4}$, is added in order to be able to calculate the denominator function, $D(s)$ [Eq. (2.5)], and the norm, $N$ [Eq. (2.7)], analytically. As our form factor, $g(k_c^2)$ of Eq. (2.9), has no singularities, the $T$ matrix of Eq. (2.4) satisfies exact two-particle unitarity.[11] This means $T$ would lead to real nucleon-nucleon scattering phase shifts for $s>4m^2$. As we do not purport, at this stage, to give a completely realistic description of the deuteron, we do not adjust our interaction to these phase shifts, as is usually done, but we will determine the two parameters in our model, the range $\Lambda$ and the strength $\lambda$ of the interaction, using the experimental values for the deuteron binding energy[17] (2.225 MeV) and the deuteron charge radius[18] (2.10 fm).

## III. THE FORM FACTOR

Having determined the deuteron vertex function, we can calculate the matrix element of the electromagnetic current and obtain the electromagnetic form factor. In the impulse approximation, shown in Fig. 2, we have

$$\begin{aligned}F_\mu(Q^2)&=\langle P+q|J_\mu|P\rangle\\&=i\int\frac{d^4k}{(2\pi)^4}\Gamma(k;P)G(k)G(P-k)(2k+q)_\mu\\&\quad\times G(k+q)\Gamma(k+q;P+q) ,\end{aligned} \tag{3.1}$$

where $Q^2=|\mathbf{q}|^2-\omega^2$ for a photon of momentum

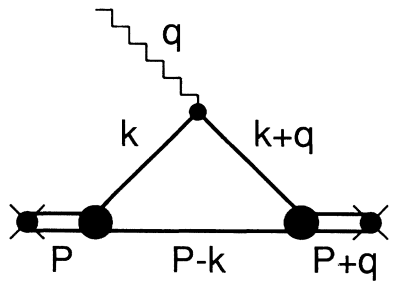


FIG. 2. The elastic electromagnetic form factor in the impulse approximation. The large filled circles denote the vertex functions, $\Gamma(k;P)$ or $\Gamma(k+q;P+q)$, and the single lines are the propagators of scalar "nucleons." The double line represents the deuteron of momentum $P$ or $P+q$, which is on its mass shell ($P^2=M^2$) both in the initial and the final state. On-mass-shell particles are denoted by the crosses.

$q=(\omega,\mathbf{q})$. In the case of elastic scattering, the final deuteron, of momentum $P+q$, stays on its mass shell, i.e., $(P+q)^2=P^2=M^2$. Therefore, the Bjorken scaling variable[19] $x\equiv Q^2/(2M\omega)$ has the value $x=1$ and the form factor is a function of $Q^2$ only.

In the above equation we approximated the photon-"nucleon" vertex by the coupling of a pointlike spin 0 "nucleon" to the photon. In a more realistic investigation of the deuteron properties one would definitely have to choose a more realistic photon-nucleon vertex, involving the correct spin structure and the form factors of the nucleon, as is done, for example, in Ref. 12. Taking into account the gauge invariance of the electromagnetic (e.m.) current matrix element, i.e., the fact that $q^\mu F_\mu(Q^2)=0$, as is demonstrated in Appendix A, we can write

$$F_\mu(Q^2)=\left[P_\mu-\frac{(P\cdot q)}{q^2}q_\mu\right]A(Q^2)\ . \tag{3.2}$$

For $Q^2=0$, the integral of Eq. (3.1) can be performed analytically,

$$F_0(Q^2=0)=N^2\frac{M}{m(4m^2-M^2)^{1/2}}\times\left[\frac{2\Lambda}{2\Lambda+(4m^2-M^2)^{1/2}}\right]^3\ . \tag{3.3}$$

As the elastic e.m. form factor reduces at $Q^2=0$ to the total charge,[12] i.e., $F_0(Q^2=0)=1$, Eq. (3.3) can be used to normalize the relativistic deuteron wave function. Another common procedure to calculate the normalization factor is to use the relation

$$N^2=\left[\frac{\partial}{\partial M}\left[\frac{D(s=M^2)-1}{\lambda}\right]\right]^{-1}\ . \tag{3.4}$$

With the specification of the covariant form factor $g(k;P)$ [Eq. (2.9)], $D(s)$ may be calculated from Eq. (2.6), with the result

$$D(s)=1+\frac{4\lambda\Lambda^3}{m[2\Lambda-i(s-4m^2)^{1/2}]^2}\ . \tag{3.5}$$

Thus $D(s)$ is real for $s<4m^2$ and has a cut in the complex $s$ plane for $s>4m^2$. Equation (3.4) leads to the same expression for the normalization factor $N$ as is obtained from the use of Eq. (3.3). For $Q^2\neq 0$, however, the calculation of $A(Q^2)$ [see Eq. (3.2)] cannot be carried out analytically and, as a consequence, we have to evaluate a three-dimensional integral numerically. We do this by making use of Gauss quadrature. In the case of integration over an infinite domain, we use Gauss points and weights on a finite interval and transform them via suitable mappings. Furthermore, the covariant form factors, $g(k_c^2)$, give rise to two branch cuts, which complicate the contour integration in the $k_0$ plane.

We could greatly simplify this calculation, if we would put the spectator nucleon of momentum $P-k$ on its mass shell, as is shown in Fig. 3. This means that in the calculation we would replace the free propagator $G(P-k)$ by the corresponding "on-shell" expression,[15] $H(P-k)$:

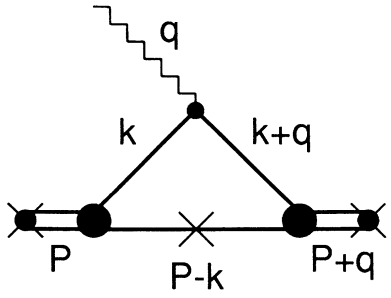


FIG. 3. The elastic electromagnetic form factor calculated in the "pole approximation." In contrast to Fig. 2, the spectator nucleon of momentum $P-k$ is now on its mass shell, as is indicated by the cross through the corresponding nucleon line.

$$G(P-k)\rightarrow H(P-k)=-2\pi i\frac{\delta(M-k_0-E(\mathbf{k}))}{2E(\mathbf{k})}\ , \tag{3.6}$$

where $E(\mathbf{k})=(|\mathbf{k}|^2+m^2)^{1/2}$. Equation (3.6) is valid in the rest frame of the deuteron, i.e., $P=(M,\mathbf{0})$. (This technique is described in Ref. 15.) In this manner we can immediately perform the $k_0$ integration and avoid the consideration of branch cuts. The elastic e.m. form factor is now strictly real, as expected.

Figure 4 shows the e.m. form factor, $F_0(Q^2)$, calculated using Eq. (3.1) (solid line) and its "on-shell-spectator" approximation calculated with Eq. (3.6) (dashed line), as functions of $Q^2$. We see that the above approximation is very good up to $Q^2\approx 5$ GeV$^2$. At about $Q^2\approx 15$ GeV$^2$, $F_0(Q^2)$ changes sign, while $F_0(Q^2)$ calculated in the "on-shell-spectator" approximation does not. This leads

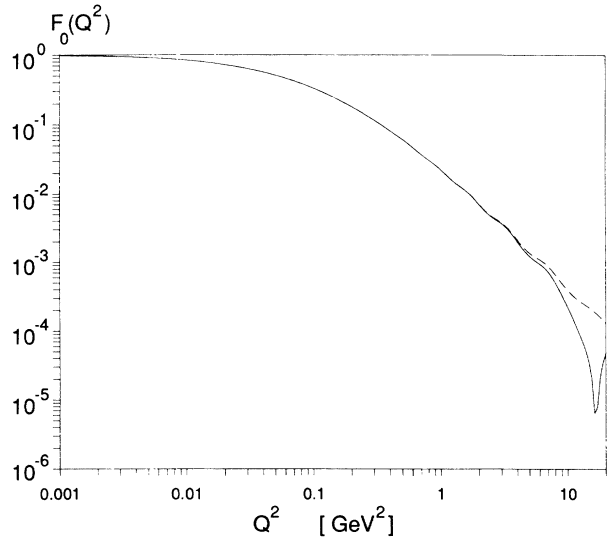


FIG. 4. The electromagnetic form factor, $F_0(Q^2)$, as a function of $Q^2$, the four-momentum transfer squared. The full line corresponds to the exact IA calculation and the dashed line corresponds to the "pole approximation," where the spectator nucleon of momentum $P-k$ is put on its mass shell, as is shown in Fig. 3.

to the deviation seen in Fig. 4, which appears in a region where the two form factors are already very small. The reason why the "on-shell-spectator" approximation of Eq. (3.6) is very good is that the major contribution to the integral of Eq. (3.1) comes from the particle pole of $G(P-k)$. We only make a very small error, if we pick up only this pole, as is done when using Eq. (3.6), and neglect the contributions coming from the poles of $G(k)$ and $G(k+q)$ or from the branch cut. The validity of this approximation is due to the highly nonrelativistic character of the bound state. In order to avoid confusion with the notion of an "off-mass-shell" form factor to be introduced shortly, we will call the use of Eq. (3.6) for the evaluation of the form factor the "pole approximation." The details of this calculation are given in Appendix B.

From the slope of the curve for $F_0(Q^2)$ vs $Q^2$ at $Q^2=0$ we can extract a value for the charge radius of the deuteron:

$$r_c^2=\left[-6\frac{\partial F_0(Q^2)}{\partial Q^2}\right]_{Q^2=0,x=1}. \tag{3.7}$$

The experimental value,[18] $r_c=2.10$ fm, fixes the range parameter $\Lambda$ of the potential to be $\Lambda=200$ MeV. With this result and using the deuteron mass $M$, which is determined by the deuteron binding energy,[17] $E_B=2.225$ MeV, we find, upon combining Eqs. (2.6) and (3.5), the parameter which specifies the strength of the potential: $\lambda=-7.23$. In this manner the two parameters of our model are fixed.

We will see in the following sections, that for the investigation of the final state interaction (FSI) we will also need the "off-shell" matrix element of the e.m. current, i.e., $F_\mu(x,Q^2)$ for $x\neq 1$ or $s\equiv(P+q)^2\neq M^2$. Such an object appears in our analysis due to the use of a separable interaction. One can see from Figs. 2 or 3, that for $s>4m^2$ both particles of momentum $P-k$ and $k+q$ can simultaneously go on their mass shells. This means that, after carrying out the $k_0$ intergration, the integrand of the integral over the angle $\theta$ has a pole in $\cos\theta$ in the domain $[-1,1]$, if (and only if) $s>4m^2$. Because we do not have an analytic expression for this integrand in the case of the "off-shell" matrix element, $F_\mu(x,Q^2)$, we cannot perform appropriate subtractions which facilitate the evaluation of the integral without ambiguity. Due to the existence of this additional pole it is therefore problematic to numerically calculate the off-shell quantity $F_\mu(x,Q^2)$ for $x\neq 1$. However, if we use the "pole approximation" of Eq. (3.6), we have an analytic expression for this integrand and we can perform a useful subtraction, using the formula

$$\int_{y-h}^{y+h}\frac{f(x)}{x-y-i\varepsilon}dx=\int_{y-h}^{y+h}\frac{f(x)-f(y)}{x-y}dx+i\pi f(y)\,. \tag{3.8}$$

This means that for $s>4m^2$ the integral over the angle $\theta$ becomes a principal value integral and, further, $F_\mu(x,Q^2)$ takes on an imaginary part, as can be seen from Eq. (3.8). Figure 5 shows the "off-shell" e.m. form factor $F_0(x,Q^2)$ calculated, using the "pole approximation" of Eq. (3.6),

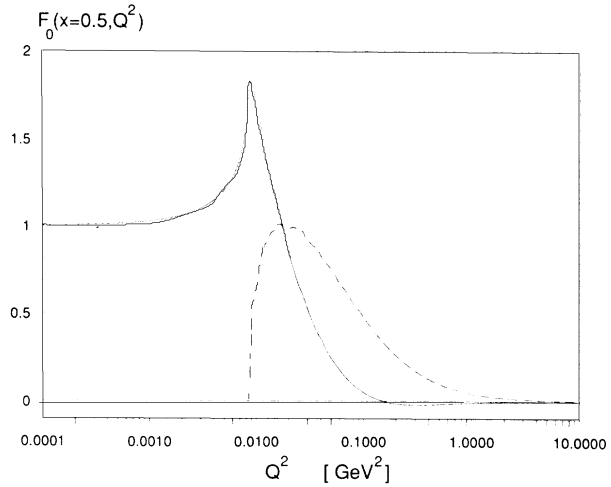


FIG. 5. The "off-shell" electromagnetic form factor, $F_0(x,Q^2)$, for $x=0.5$, calculated using the "pole approximation" as a function of the momentum transfer, $Q^2$. The full line corresponds to the real part of $F_0$, while the dashed line represents the imaginary part.

as described above, for $x\equiv Q^2/(2M\omega)=0.5$, as a function of $Q^2$. The imaginary part of $F_0(x,Q^2)$, the dashed line, is identically zero for $s<4m^2$ or $Q^2<x(4m^2-M^2)/(1-x)$. This means that for elastic scattering, i.e., $x=1$, $F_\mu(x,Q^2)$ is real for all $Q^2$.

## IV. THE HADRONIC TENSOR IN PLANE WAVE IMPULSE APPROXIMATION

In this section we will consider inclusive inelastic unpolarized electron-"deuteron" scattering. We again use the impulse approximation and neglect the spin of the nucleons and the deuteron. The process to be discussed is illustrated in Fig. 6. The corresponding cross section may be written as[20]

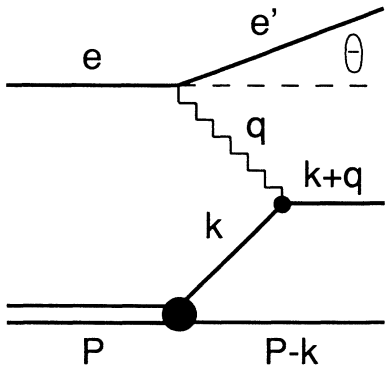


FIG. 6. Inelastic electron-deuteron scattering in the one-photon exchange approximation. The four-momentum of the virtual photon is $q=(\omega,\mathbf{q})$. The deuteron momentum is $P$; the spectator nucleon has momentum $P-k$ and the struck nucleon has momentum $k$ before and $k+q$ after the absorption of the photon.

$$\frac{d^2\sigma}{dE'd\Omega}=\left[\frac{d\sigma}{d\Omega}\right]_M\left[W_2(Q^2,x)+2W_1(Q^2,x)\tan^2\left[\frac{\theta}{2}\right]\right], \quad (4.1)$$

where $E'$ is the energy of the final electron, $\theta$ is the scattering angle, and

$$\left[\frac{d\sigma}{d\Omega}\right]_M=\frac{4\alpha^2E'^2}{Q^4}\cos^2\left[\frac{\theta}{2}\right] \quad (4.2)$$

is the well-known Mott cross section[21] for the scattering of relativistic electrons in the Coulomb field of a spin 0 particle with infinite mass.[22] The Lorentz-invariant structure functions, $W_1$ and $W_2$, depend on the two scalar variables, $Q^2=|\mathbf{q}|^2-\omega^2$, the squared four-momentum transfer, and $x=Q^2/(2P\cdot q)$, the Bjorken scaling variable,[19] which reduces to $x=Q^2/(2M\omega)$ in the rest frame of the deuteron. Here $\omega=E-E'$ is the energy loss of the electron and $q=(\omega,\mathbf{q})$ is the four-momentum of the exchanged photon. In this case the photon of four-momentum $q$ is spacelike, so that $Q^2\equiv -q^2>0$.

The structure functions specify the symmetric part of the hadronic tensor $W_{\mu\nu}$,[20]

$$W_{\mu\nu}=-\left[g_{\mu\nu}-\frac{q_\mu q_\nu}{q^2}\right]W_1(Q^2,x)+\hat{P}_\mu\hat{P}_\nu\frac{W_2(Q^2,x)}{M^2}, \quad (4.3)$$

where $\hat{P}_\mu=[P_\mu-(P\cdot q)q_\mu/q^2]$. No other terms appear in Eq. (4.3) due to Lorentz invariance, current conservation ($q^\mu W_{\mu\nu}=W_{\mu\nu}q^\nu=0$), and parity invariance.[20] It is the goal of this section to calculate the spin-independent structure functions, $W_1$ and $W_2$, and the hadronic tensor, $W_{\mu\nu}$, in the plane wave impulse approximation (PWIA). That is, we neglect the effects of the final state interaction (FSI). In Sec. VI these effects will be taken into account and we will see how they modify $W_{\mu\nu}$.

The hadronic tensor can be expressed as an integral over the expectation value in the deuteron ground state of the e.m. current commutator:

$$W_{\mu\nu}=\frac{1}{2\pi}\int d^4x\, e^{iq\cdot x}\langle P_D|[J_\mu(x),J_\nu(0)]|P_D\rangle . \quad (4.4)$$

The amplitude, $W_{\mu\nu}$, is proportional to the discontinuity across the cut along the line $\omega>0$, of the forward virtual Compton scattering amplitude,[23] $T_{\mu\nu}$, where

$$T_{\mu\nu}=i\int d^4x\, e^{iq\cdot x}\langle P_D|T[J_\mu(x)J_\nu(0)]|P_D\rangle . \quad (4.5)$$

In Eq. (4.5) the current commutator of Eq. (4.4) is replaced by a time-ordered product. In the plane wave impulse approximation (PWIA), depicted in Fig. 7, we have

$$W_{\mu\nu}=-\frac{1}{2\pi}\int\frac{d^4k}{(2\pi)^4}\Gamma^2(k;P)G^2(k)(2k+q)_\mu\times(2k+q)_\nu H(P-k)H(k+q) . \quad (4.6)$$

In addition to the free [Eq. (2.2)] and "on-shell" propagators [Eq. (3.6)], Eq. (4.6) involves the deuteron vertex function $\Gamma(k;P)$ [Eq. (2.7)], calculated in Sec. II. In deriving Eq. (4.6) from Eq. (4.4) we further replaced the actual e.m. current by the current of free pointlike scalar particles. Clearly this is an approximation.

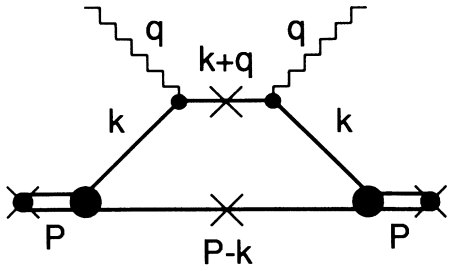


FIG. 7. The hadronic tensor $W_{\mu\nu}$ in the plane wave impulse approximation (PWIA). The large filled circle denotes the deuteron vertex function, $\Gamma(k;P)$; the single lines stand for the propagators of scalar "nucleons" and the double line represents the deuteron. The crosses indicate that the corresponding particle is on its mass shell.

We proceed by projecting out the structure functions $W_1$ and $W_2$ using the identities

$$\hat{P}^\mu\hat{P}^\nu W_{\mu\nu}=-\gamma M^2W_1+\gamma^2M^2W_2 , \quad (4.7a)$$

$$\left[g^{\mu\nu}-\frac{q^\mu q^\nu}{q^2}\right]W_{\mu\nu}=-3W_1+\gamma W_2 . \quad (4.7b)$$

Here $\gamma M^2\equiv\hat{P}_\mu\hat{P}^\mu=M^2-(P\cdot q)^2/q^2$. Solving for the structure functions we find

$$W_{1,2}=-\frac{1}{2\pi}\int\frac{d^4k}{(2\pi)^4}\Gamma^2(k;P)G^2(k)\times w_{1,2}H(P-k)H(k+q) , \quad (4.8)$$

with the kernels

$$w_1=2\left[\left[(P\cdot k)-\frac{(P\cdot q)(k\cdot q)}{q^2}\right]^2\Big/(\gamma M^2)-\left[k^2-\frac{(k\cdot q)^2}{q^2}\right]\right], \quad (4.8a)$$

and

$$w_2=\left[3w_1+4\left[k^2-\frac{(k\cdot q)^2}{q^2}\right]\right]\Big/\gamma . \quad (4.8b)$$

Up to this point we have not chosen a special Lorentz frame and all our expressions are fully covariant. In order to continue with our analysis, we have to specify a reference frame. We choose the rest frame of the deuteron, i.e., $P=(M,\mathbf{0})$. The use of the "on-shell" propagator, $H(P-k)$ [see Eq. (3.6)],

$$H(P-k)=-2\pi i\frac{\delta(M-k_0-E(\mathbf{k}))}{2E(\mathbf{k})} , \quad (4.9)$$

where $E(\mathbf{k})=(|\mathbf{k}|^2+m^2)^{1/2}$, eliminates the $k_0$ integration in Eq. (4.8). The "on-shell" propagator,

$$H(k+q)=-2\pi i\frac{\delta(k_0+\omega-E(\mathbf{k}+\mathbf{q}))}{2E(\mathbf{k}+\mathbf{q})}\ , \tag{4.10a}$$

where $E(\mathbf{k}+\mathbf{q})=(|\mathbf{k}+\mathbf{q}|^2+m^2)^{1/2}$, restricts the angle between the photon momentum $\mathbf{q}$ and the integration variable $\mathbf{k}$ and thus leads to the presence of a $\delta$ function in the variable $\cos\theta$:

$$H(k+q)=-\frac{\pi i}{|\mathbf{k}||\mathbf{q}|}\delta\left[\cos\theta-\frac{s-2(M+\omega)E(\mathbf{k})}{2|\mathbf{k}||\mathbf{q}|}\right]\ . \tag{4.10b}$$

This eliminates the integration over $\cos\theta$ in Eq. (4.8). Because we must require that $|\cos\theta|<1$, this $\delta$ function further leads to a constraint in the $|\mathbf{k}|$ integration, i.e., it restricts the range of the integration over $|\mathbf{k}|$:

$$\int_0^\infty d|\mathbf{k}|\rightarrow\int_a^b d|\mathbf{k}|\ , \tag{4.11}$$

with

$$a=\tfrac{1}{2}\left|(M+\omega)\left[1-\frac{4m^2}{s}\right]^{1/2}-|\mathbf{q}|\right| \tag{4.11a}$$

and

$$b=\tfrac{1}{2}\left[(M+\omega)\left[1-\frac{4m^2}{s}\right]^{1/2}+|\mathbf{q}|\right]\ . \tag{4.11b}$$

Here $s=M^2+2M\omega-Q^2$.

If we now define the dimensionless structures functions,[20]

$$F_1(Q^2,x)=MW_1(Q^2,x)\ , \tag{4.12a}$$

$$F_2(Q^2,x)=\omega W_2(Q^2,x)\ , \tag{4.12b}$$

we finally obtain from Eq. (4.8), using Eqs. (4.9)–(4.11),

$$F_1(Q^2,x)=\left[\frac{N}{2\pi}\right]^2\int_a^b\frac{|\mathbf{k}|^2d|\mathbf{k}|}{2E(\mathbf{k})}g^2(|\mathbf{k}|^2)G^2(k)w_1'\ , \tag{4.13a}$$

and

$$F_2(Q^2,x)=6x\frac{\omega^2}{|\mathbf{q}|^2}F_1(Q^2,x)+\left[\frac{N}{2\pi}\right]^2\int_a^b\frac{|\mathbf{k}|^2d|\mathbf{k}|}{2E(\mathbf{k})}g^2(|\mathbf{k}|^2)G^2(k)w_2'\ . \tag{4.13b}$$

Here the kernels $w_1'$ and $w_2'$ are

$$w_1'=\frac{M|\mathbf{k}|}{|\mathbf{q}|}\left[1-\left[\frac{s-2(M+\omega)E(\mathbf{k})}{2|\mathbf{k}||\mathbf{q}|}\right]^2\right]\ , \tag{4.14a}$$

and

$$w_2'=\frac{\omega}{2|\mathbf{k}||\mathbf{q}|^3}\{4m^2Q^2+[M^2+Q^2-2ME(\mathbf{k})]^2\}\ , \tag{4.14b}$$

where $E(\mathbf{k})=(|\mathbf{k}|^2+m^2)^{1/2}$. $N$ is the normalization factor of the deuteron wave function, calculated in Sec. III, and $G(k)=1/[M^2-2ME(\mathbf{k})]$ [see Eq. (4.9)]. For the covariant vertex function, $g(k_c^2)$, we take the expression given in Eq. (2.9), where $k_c^2$ is replaced by $|\mathbf{k}|^2$, since we are working in the rest frame of the deuteron. The integrals of Eq. (4.13) are carried out numerically, again using Gaussian quadrature. The results of these computations will be exhibited and discussed in Sec. VIII. It should be noted that below the elastic threshold, where the target stays intact and only recoils, the structure functions necessarily vanish. Thus, for

$$s\equiv M^2+2M\omega-Q^2<4m^2\ , \tag{4.15}$$

$F_1(Q^2,x)=F_2(Q^2,x)=0$. The condition expressed by Eq. (4.15) can be derived from Eq. (4.10b), because only if $s>4m^2$, can the $\delta$ function contribute to the integral. If we express Eq. (4.15) in terms of the Bjorken scaling variable, $x$, and keep in mind that $x$ is by definition positive, we get

$$0<x<\frac{Q^2}{4m^2-M^2+Q^2}<1\ . \tag{4.16}$$

This shows that our model leads to the proper support for the structure functions, i.e., $0<x<1$.

## V. $x$ SCALING AND SUM RULES

In this section we investigate the asymptotic behavior of the structure functions, $F_1(Q^2,x)$ and $F_2(Q^2,x)$, in the deep-inelastic or Bjorken limit, where $Q^2\rightarrow\infty$ and $\omega\rightarrow\infty$, for finite $x$. In this context it is not necessary to take the final state interaction into account, because the corrections to $F_1$ and $F_2$ coming from the FSI vanish for large $Q^2$, as will be seen in the next section. We can therefore use the PWIA expressions [Eq. (4.13)] for $F_1$ and $F_2$, which have been derived in Sec. IV.

We shall show that our model exhibits Bjorken scaling.[24] That is, in the deep-inelastic limit, the dimensionless structure functions become functions of a single, dimensionless variable, $x$,

$$F_{1,2}(Q^2,x)\rightarrow F_{1,2}(x)\ . \tag{5.1}$$

We shall further show that our model obeys a Callan-Gross relation,[25] which, in the case of scalar particles, is[22]

$$F_1(x)\equiv 0\ . \tag{5.2}$$

We will also demonstrate that the "Coulomb sum rule,"

$$\int_0^1 dx\frac{F_2(x)}{x}=1\ , \tag{5.3}$$

is satisfied. In the following all expressions will be given up to leading order in $1/Q^2$ only.

We start with the kernels [Eq. (4.14)] of the integrals of Eq. (4.13). In the Bjorken limit they take the form

$$w_1'\rightarrow\frac{2M^2x}{|\mathbf{k}|Q^2}[2M(1-x)E(\mathbf{k})-M^2(1-x)^2-m^2] \tag{5.4a}$$

and

$$w_2'\rightarrow\frac{2M^2x^2}{|\mathbf{k}|}\ . \tag{5.4b}$$

The only other terms in Eq. (4.13), which depend on the photon momentum, are the limits of integration $a$ and $b$, given in Eq. (4.11). We find

$$a \to a(x) = \frac{1}{2}\left| \frac{m^2}{M(1-x)} - M(1-x) \right| \tag{5.5a}$$

and

$$b \to \frac{Q^2}{2Mx} \to \infty \ . \tag{5.5b}$$

As the kernel for $F_1(Q^2,x)$ decreases as $1/Q^2$ with increasing $Q^2$, we see that $F_1(x)$ vanishes in the Bjorken limit. Thus, our model satisfies the Callan-Gross relation for scalar particles [Eq. (5.2)], while $F_2(Q^2,x)$ stays finite and exhibits scaling behavior, i.e., $F_2(Q^2,x) \to F_2(x)$. We have for $Q^2 \to \infty$,

$$F_1(Q^2,x) \to F_1(x) = 0 \tag{5.6a}$$

and

$$F_2(Q^2,x) \to F_2(x) = \left[ \frac{N}{2\pi} \right]^2 \int_{a(x)}^{\infty} \frac{|\mathbf{k}|^2 d|\mathbf{k}|}{2E(\mathbf{k})} g^2(|\mathbf{k}|^2) \times G^2(k) \frac{2M^2x^2}{|\mathbf{k}|} \ . \tag{5.6b}$$

Using Eq. (5.6b), we can explicitly calculate the moments of $F_2(x)$, defined as

$$I_n = \int_0^1 dx\, x^n F_2(x) \ . \tag{5.7}$$

In some cases such expressions can be related to matrix elements of the vector or axial vector current and we obtain sum rules. In the case of spinless particles we can only derive a single sum rule. Before we can perform the integration over $x$ in Eq. (5.7) we have to go through some algebra. It is a simple exercise to show that for every integrable function $A(x,|\mathbf{k}|)$,

$$\int_{-\infty}^{1} dx \int_{a(x)}^{\infty} d|\mathbf{k}|\, A(x,|\mathbf{k}|) = \int_0^{\infty} d|\mathbf{k}| \int_u^v dx\ A(x,|\mathbf{k}|) \ , \tag{5.8}$$

where we have used Eq. (5.5a) and defined

$$u = u(|\mathbf{k}|) = \frac{M - E(\mathbf{k}) - |\mathbf{k}|}{M} \tag{5.9a}$$

and

$$v = v(|\mathbf{k}|) = \frac{M - E(\mathbf{k}) + |\mathbf{k}|}{M} \ . \tag{5.9b}$$

If we keep in mind that $F_2(x)$ is strictly zero for $x < 0$, we see that we can extend the range of the $x$ integration in Eq. (5.7) to $-\infty$. We finally obtain for the moments, $I_n$, of $F_2(x)$

$$I_n = \left[ \frac{N}{2\pi} \right]^2 \int_0^{\infty} \frac{|\mathbf{k}|^2 d|\mathbf{k}|}{2E(\mathbf{k})} g^2(|\mathbf{k}|^2) G^2(k) \times \int_u^v dx \frac{2M^2x^{n+2}}{|\mathbf{k}|} \ , \tag{5.10}$$

with $E(\mathbf{k}) = (|\mathbf{k}|^2 + m^2)^{1/2}$. The limits of integration, $u$ and $v$, are given in Eq. (5.9). For $I_{-1}$ we have

$$I_{-1} = 2 \left[ \frac{N}{2\pi} \right]^2 \int_0^{\infty} \frac{|\mathbf{k}|^2 d|\mathbf{k}|}{2E(\mathbf{k})} g^2(|\mathbf{k}|^2) G^2(k) \times 2[M - E(\mathbf{k})] \ . \tag{5.11}$$

If we recall the work of Sec. III, we see that this is exactly the elastic form factor $F_0(Q^2)$, for $Q^2 = 0$, calculated in the "pole approximation." To verify this, we just use the approximation of Eq. (3.6) in Eq. (3.1) and find

$$F_0(Q^2 = 0) = i \int \frac{d^4k}{(2\pi)^4} \Gamma(k;P) G(k) H(P-k) \times 2k_0 G(k) \Gamma(k;P) \ . \tag{5.12}$$

If we evaluate this integral in the deuteron rest frame [use Eqs. (4.9) and (2.7)], we see that the integrand is independent of the polar and azimuthal angles and that Eq. (5.12) reduces to Eq. (5.11).

The integral of Eq. (5.11) can only be evaluated numerically. The result is that $F_0(Q^2 = 0)$, calculated from Eq. (5.11), deviates only in the fourth digit from 1, the value of $F_0(Q^2 = 0)$ specified for a calculation done without making the "pole approximation" of Eq. (3.6). This choice, $F_0(Q^2 = 0) = 1$, was used to normalize the deuteron wave function. Therefore, our model satisfies the "Coulomb sum rule"

$$\int_0^1 dx \frac{F_2(x)}{x} = F_0(Q^2 = 0) = 1 \ , \tag{5.13}$$

where the e.m. form factor $F_0(Q^2 = 0)$ is calculated in the "pole approximation" of Eq. (3.6), i.e., by putting the spectator nucleon on shell. (See Fig. 3.) We stress that our ability to derive this sum rule in the PWIA is based upon the accuracy of the "pole approximation" in the calculation of the form factor $F_0(Q^2 = 0)$. The accuracy of that approximation depends upon the nonrelativistic nature of the bound state considered here, as mentioned earlier.

We end this section by pointing out that all the results presented in this section are independent of the specific choice made for the deuteron wave function, as long as we use a separable rank-one interaction.

## VI. THE EXACT CALCULATION FOR THE HADRONIC TENSOR INCLUDING FSI

In the plane wave impulse approximation, described in Sec. IV, we neglected the interaction between the spectator nucleon and the nucleon which absorbed the photon, as can be seen from Fig. 7. Clearly this is an approximation, because any interaction between these two particles would modify the response of the system to the external probe. We may take this final state interaction (FSI) into account by using distorted waves, as is depicted in Fig. 8.

(In previous publications[26,27] it was shown that inserting a wave operator $\Omega$ into a reduced Feynman graph is equivalent to the use of distorted instead of plane waves.) Now the spectator nucleon, of momentum $P-k'$, and the struck nucleon, of momentum $k'+q$, undergo an interaction described by the wave operator $\Omega$, before they are put on their mass shells. It is obvious that in the construction of $\Omega$ we have to use the same separable rank-one interaction, i.e., the same $T$ matrix, which we used for the construction of the deuteron bound state. This leads to our writing $\Omega=1+GGT$, with $T$ taken from Eq. (2.4). More specially,

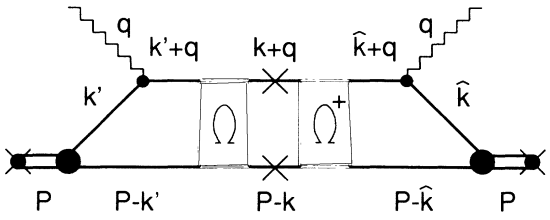


FIG. 8. The exact calculation for the hadronic tensor $W_{\mu\nu}$. The wave operator, $\Omega$ contains the final state interactions (FSI) between the spectator nucleon and the struck nucleon.

$$\Omega(k'+q,k+q;P+q)=(2\pi)^4\delta(k'-k)+i\frac{\lambda G(k'+q)G(P-k')g(k'+q;P+q)g(k+q;P+q)}{D(s)}\ , \tag{6.1}$$

where $s\equiv(P+q)^2$ is the invariant mass, $D(s)$ is the denominator function [Eq. (3.5)], $g$ is the covariant form factor [Eq. (2.9)], and $G$ is the Green's function for a free spin 0 particle [Eq. (2.2)].

If we make use of the wave operator, as indicated in Fig. 8, we find that two more Feynman diagrams contribute to $W_{\mu\nu}$, in addition to the one already shown in Fig. 7 and calculated in Sec. IV. These additional diagrams are depicted in Figs. 9(a) and 9(b). They lead to the following corrections in $W_{\mu\nu}$:

$$\Delta_a W_{\mu\nu}=\frac{1}{N^2}\left[\frac{\lambda}{D(s)}\hat{P}_\mu A(Q^2,x)\hat{P}_\nu B(Q^2,x)+\frac{\lambda}{D^*(s)}\hat{P}_\mu B(Q^2,x)\hat{P}_\nu A^*(Q^2,x)\right] \tag{6.2a}$$

for the process shown in Fig. 9(a) and

$$\Delta_b W_{\mu\nu}=\frac{1}{N^2}\frac{\lambda^2}{|D(s)|^2}\hat{P}_\mu A(Q^2,x)E(Q^2,x)\hat{P}_\nu A^*(Q^2,x) \tag{6.2b}$$

for the process shown in Fig. 9(b). Here we have used the following notation: $\hat{P}_\mu A(Q^2,x)\equiv F_\mu(Q^2,x)$, where $A(Q^2,x)$ is an "off-shell inelastic e.m. form factor," defined for $x\neq1$. As already discussed in Sec. III, it is not possible to make an accurate calculation of this form factor without using the "pole approximation" [Eq. (3.6)]; that is, we had to put the spectator nucleon of momentum $P-k$ on mass shell. However, it was shown in Sec. III that this is an excellent approximation up to very high $Q^2$. Thus for $A(Q^2,x)$ we find

$$A=i\int\frac{d^4k}{(2\pi)^4}\Gamma(k;P)G(k)H(P-k)\frac{2\left[(P\cdot k)-\dfrac{(P\cdot q)(k\cdot q)}{q^2}\right]}{\gamma M^2}G(k+q)\Gamma(k+q;P+q)\ , \tag{6.3}$$

where $\gamma M^2$ is defined after Eq. (4.7) and all other terms in Eq. (6.3) were previously discussed in Sec. III.

We may also define a "doubly-on-shell inelastic e.m. form factor," $B(Q^2,x)$, where

$$B=\frac{-1}{2\pi}\int\frac{d^4k}{(2\pi)^4}\Gamma(k;P)G(k)H(P-k)\frac{2\left[(P\cdot k)-\dfrac{(P\cdot q)(k\cdot q)}{q^2}\right]}{\gamma M^2}H(k+q)\Gamma(k+q;P+q)\ . \tag{6.4}$$

This quantity is calculated in analogy to Eq. (6.3); the only difference is that in Eq. (6.4) the particle of momentum $k+q$ is also on its mass shell.

Finally, $E(Q^2,x)$ may be called the "doubly-on-shell denominator function," calculated in analogy to $[1-D(s)]/\lambda$ [see (2.5)], but again with both intermediate nucleons on their mass shells. This yields

$$E(Q^2,x)=\frac{-1}{2\pi}\int\frac{d^4k}{(2\pi)^4}g(k+q;P+q)H(k+q)H(P-k)g(k+q;P+q)\ . \tag{6.5}$$

In Eqs. (6.4) and (6.5) the same combination of $\delta$ functions occurs as in the calculation of the structure functions in the PWIA, i.e., in Eq. (4.8). This leads to the same kinematical constraints as those found in Sec. IV, i.e., $s>4m^2$ and a restriction for the $|\mathbf{k}|$ integration with the limits given in Eq. (4.11). Using these results, Eqs. (6.4) and (6.5) reduce to simple one-dimensional integrals, which are evaluated in the deuteron rest frame by means of Gaussian quadrature.

From Eq. (6.2) we see that the FSI corrections to $W_{\mu\nu}$ contribute only in $F_2(Q^2,x)$. If we analyze the asymptotic behavior of these corrections in the deep-inelastic limit,

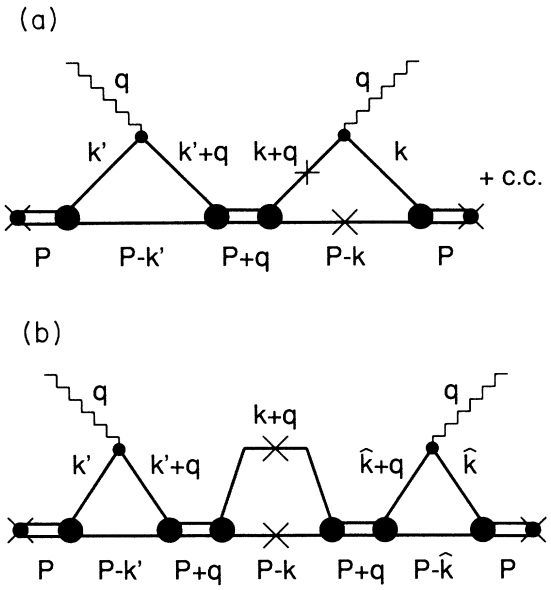


FIG. 9. Additional Feynman diagrams for the calculation of the hadronic tensor $W_{\mu\nu}$ arising from the FSI between the spectator and the struck nucleon. The diagrams exhibit a factorization property due to the separable nature of our interaction. The double line, labeled $P+q$, represents an intermediate *off-shell* "deuteron" bound state, formed by the struck and the spectator nucleon, before they are put on their mass shells (as is indicated by the crosses). The appearance of this bound state arises through the presence of the $T$ matrix in the wave operator $\Omega$ [see Eq. (6.1)]; the structure of the diagrams is again due to the separable nature of the interaction and gives rise to the necessity of calculating "off-mass-shell" form factors, $F_\mu(x,Q^2)$, as described in Sec. III.

we find that the extra terms in $F_2(Q^2,x)$ decrease with $Q^2$ as $(1/Q^2)^{5/2}$, $(1/Q^2)^4$, and $(1/Q^2)^5$, respectively. This shows that the FSI corrections vanish very fast with increasing $Q^2$ and that they therefore do not contribute to the structure functions in the Bjorken scaling limit. These terms, however, modify the approach to scaling. This will be discussed in Sec. VIII, where we present the results of our numerical calculations.

The fact that the FSI corrections vanish with these unusually high powers of $1/Q^2$ was also observed by Rosenfelder[28] for the case of a nonrelativistic separable interaction. In our case it is due to the factorization property of the diagram in Fig. 8 and therefore to the separability of the interaction used. It would be interesting to study the behavior of the FSI at large $Q^2$ in a calculation which does not make a separable Ansatz for the interaction.

## VII. $y$ SCALING

In the preceding sections we expressed the response of the deuteron to the virtual photon in terms of the structure functions, $F_1$ and $F_2$, which, in general, are functions of $Q^2$, the four-momentum transfer squared, and the Bjorken scaling variable $x \equiv Q^2/(2M\omega)$. This notation was adopted from deep-inelastic electron-nucleon scattering, where the momentum transfer is in excess of several GeV and where the virtual photon probes the parton substructure of the nucleon.[20] However, we are here interested in quasielastic electron-deuteron scattering, where the momentum transfer, although large, is much smaller than in the deep-inelastic regime. It is, therefore, appropriate to change to another description.

It was predicted by West,[1] and later observed by others,[2] that in this case the reduced cross section, $F(Q^2,y)$, scales in terms of a variable $y$. However, the proper definition of both the scaling function, $F(y)$, and the scaling variable, $y$, have been the subject of extensive discussions.[3] The fact that different authors used different scaling variables and functions leads to considerable confusion. In this investigation we shall follow the notation favored by Butler and McKeown.[3]

According to the $y$-scaling hypothesis, in the impulse approximation the differential cross section for lepton-nucleus quasielastic scattering can be written as[3,4]

$$\frac{d^2\sigma}{dE'd\Omega} = \left[ Z\left[\frac{d\sigma}{d\Omega}\right]_p + N\left[\frac{d\sigma}{d\Omega}\right]_n \right] \frac{m}{|\mathbf{q}|} F(Q^2,y) \ . \quad (7.1)$$

In this expression $E'$ is the final electron energy, $Z(N)$ is the proton (neutron) number of the target, and $\{d\sigma/d\Omega\}_{p(n)}$ is the elastic electron-proton (neutron) cross section.

In the simple impulse approximation $F(Q^2,y)$ is related to the nucleon momentum distribution[5] $n(p)$:

$$F(Q^2,y) = \frac{1}{(2\pi)^2} \int_a^b pn(p)dp \ . \quad (7.2)$$

The limits of the integration, $a$ and $b$, arise from the energy-conserving $\delta$ function, which is also the origin of the factor $m/|\mathbf{q}|$ in Eq. (7.1). As $|\mathbf{q}|$ becomes larger and larger, the upper limit $b$ tends towards infinity and the integral of Eq. (7.2) becomes a function solely of $a$, which we will now call $|y|$.

$$F(Q^2,y) \rightarrow F(y) = \frac{1}{(2\pi)^2} \int_{|y|}^{\infty} pn(p)dp \ . \quad (7.3)$$

However, the definition of $y$, which depends on the form of the energy-conserving $\delta$ function, hinges on the kinematics of the model. There are a number of options: relativistic or nonrelativistic kinematics; inclusion or neglect of recoil, binding effects and/or excitation of the core, etc. With the choice of relativistic kinematics, we may specify energy conservation, in the case of electron-deuteron scattering, using the relations

$$\omega + M = (|\mathbf{p}+\mathbf{q}|^2 + m^2)^{1/2} + (|\mathbf{p}|^2 + m^2)^{1/2} \ . \quad (7.4)$$

Here $\mathbf{p}+\mathbf{q}$ is the three-momentum of the struck nucleon after the absorption of the photon and $-\mathbf{p}$ is the momentum of the recoiling spectator nucleon, whose excitation is neglected. This leads to

$$p_{\min} \equiv a = \frac{1}{2} \left| (M+\omega) \left[ 1 - \frac{4m^2}{s} \right]^{1/2} - |\mathbf{q}| \right| , \quad (7.5a)$$

$$p_{\max} \equiv b = \frac{1}{2} \left[ (M+\omega) \left[ 1 - \frac{4m^2}{s} \right]^{1/2} + |\mathbf{q}| \right] . \quad (7.5b)$$

These are exactly the same limits of integration as we found for the structure functions in the PWIA in Sec. IV. [See Eq. (4.11).] Thus, the scaling variable $y$ is defined as

$$y=\frac{1}{2}\left[(M+\omega)\left[1-\frac{4m^2}{s}\right]^{1/2}-|\mathbf{q}|\right]. \tag{7.6}$$

This $y$ differs from West's[1] original scaling variable $y_W$ which is the minimum value of the three-momentum of the nucleon which absorbs the virtual photon. This nucleon is on its mass shell initially and in the final state in the West[1] analysis and nonrelativistic kinematics are used.[6,28]

It can be seen from Eq. (7.3) that the reduced cross section, $F(y)$, is maximal for $y=0$. This is the so-called quasielastic peak. The region of physical interest, however, is the domain $y<0$, where the energy transfer to the nucleon is small enough so that we may neglect pion production.[6] Furthermore, Eq. (7.5) shows that the $y$-scaling limit is the same as the Bjorken limit, where $Q^2\to\infty$, but $Q^2/\omega$ stays finite. Only in that case does the upper limit of the integration, $b$, tend to infinity, while the lower limit, $a=|y|$, stays finite. In that case Eq. (7.3) is valid and Eq. (7.6) reads

$$y=\frac{1}{2}\left[M(1-x)-\frac{m^2}{M(1-x)}\right]. \tag{7.6a}$$

After having defined the scaling variable $y$ in terms of $Q^2$ and $x$, we will now determine the scaling function $F(Q^2,y)$. If we compare Eqs. (4.1) and (7.1), we see that the reduced cross section, $F(Q^2,y)$, can be expressed in terms of the structure functions $F_1(Q^2,x)$ and $F_2(Q^2,x)$,

$$F(Q^2,y)=(Z\sigma_p+N\sigma_n)^{-1}\frac{1}{m}\times\left[\frac{|\mathbf{q}|}{\omega}F_2(Q^2,x)+\frac{2|\mathbf{q}|}{M}F_1(Q^2,x)\tan^2\left[\frac{\theta}{2}\right]\right]. \tag{7.7}$$

Here we have used the reduced nucleon cross sections,

$$\sigma_{p,n}=\left[\frac{d\sigma}{d\Omega}\right]_{p,n}\Big/\left[\frac{d\sigma}{d\Omega}\right]_M, \tag{7.8}$$

where $(d\sigma/d\Omega)_{p,n}$ is again the elastic electron-nucleon cross section and $(d\sigma/d\Omega)_M$ is the Mott cross section.

Equation (7.7) shows that in the scaling function, $F(Q^2,y)$, the spin-dependent dynamics of the nucleon and the nucleon form factor are somehow divided out, as they contribute both to the structure functions, $F_1$ and $F_2$, and to the reduced nucleon cross sections $\sigma_{p,n}$. Therefore, our simple model, where we neglected the spin and the form factors of the nucleons, might be a reasonable approximation in this case. Our model yields $\sigma_p=1$ and $\sigma_n=0$ and Eq. (7.7) then reads

$$F(Q^2,y)=\frac{1}{m}\left[\frac{|\mathbf{q}|}{\omega}F_2(Q^2,x)+\frac{2|\mathbf{q}|}{M}F_1(Q^2,x)\tan^2\left[\frac{\theta}{2}\right]\right]. \tag{7.9}$$

In the next section we will see that the kinematical factor $|\mathbf{q}|/\omega$ in Eq. (7.9) plays a very crucial role in the different approach to scaling observed in the $y$- and $x$-scaling regime.

## VIII. NUMERICAL RESULTS AND DISCUSSION

Before we discuss the topic of $y$ scaling and the effects due to the final state interaction (FSI), we will first present our results for the structure functions, $F_1(Q^2,x)$ and $F_2(Q^2,x)$, calculated in the plane wave impulse ap-

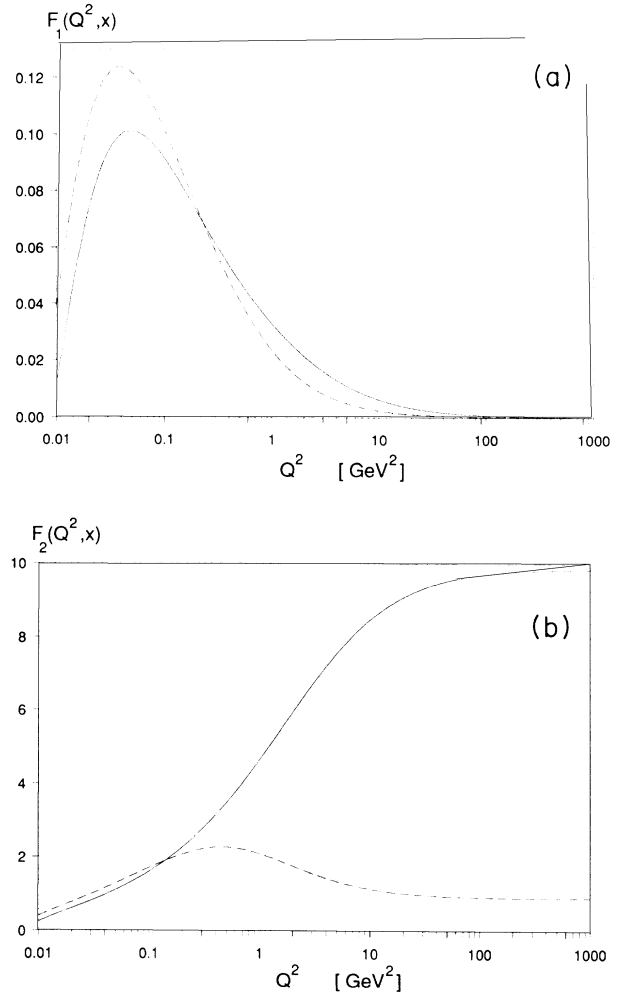


FIG. 10. The dimensionless structures functions, $F_1(Q^2,x)$ (a) and $F_2(Q^2,x)$ (b), are shown as functions of $Q^2$, the four-momentum transfer squared, for fixed values of the Bjorken scaling variable $x$. The dashed line corresponds to $x=0.45$, the full line corresponds to $x=0.50$, and the dotted line corresponds to $x=0.55$. The calculations were carried out in PWIA, i.e., the FSI between the struck and the spectator nucleon was neglected.

proximation (PWIA), as described in Sec. IV. Figure 10(a) shows the dimensionless structure function $F_1(Q^2,x)$ [Eq. (4.13a)] vs $Q^2$, the magnitude of the squared four-momentum transfer, for fixed values of the Bjorken scaling variable $x$. Figure 10(b) shows $F_2(Q^2,x)$ [Eq. (4.13b)] as a function of $Q^2$ for fixed $x$.

As already noted in Sec. V, $F_1(Q^2,x)$ vanishes in the scaling limit, i.e., for $Q^2\rightarrow\infty$ and fixed $x$. This is due to the spin 0 nature of our "nucleons." Since $F_1$ is a purely transverse structure function,[29] it is related to the photoabsorption cross section for photons of helicity $\pm1$. Such photons cannot be absorbed by spin 0 particles with collinear momentum.[20] $F_2(Q^2,x)$ stays finite in the deep-inelastic limit and exhibits scaling behavior. However, it does not reach its asymptotic value, $F_2(x)$, until $Q^2\approx100$ GeV$^2$, as can be seen from Fig. 10(b). This is far above the kinematical domain where quasielastic electron-deuteron scattering experiments are carried out ($Q^2\approx1-10$ GeV$^2$). This implies that the experimental data should not scale at all in terms of the variable $x$.

Figure 11 shows $F_2(Q^2,x)$ vs $x$ for four different values of the momentum transfer, $Q^2$, lying between 0.1 and 100 GeV$^2$. With increasing momentum transfer, the response of the deuteron to the virtual photon is more and more dominated by a sharp peak at $x\approx\frac{1}{2}$. This so-called quasielastic peak (QEP) results from quasifree scattering from individual, moving nucleons[7] and it can be used to extract an average Fermi momentum as well as the nucleon effective mass.[30]

It was shown in Sec. V that our model satisfies a "Coulomb sum rule" in the Bjorken limit,

$$I_{-1}\equiv\int_0^1 dx\frac{F_2(x)}{x}=1\ . \tag{8.1}$$

In order to investigate the effects due to the final state interaction (FSI) on the structure function $F_2(Q^2,x)$, we now define the quantity

$$I_{-1}(Q^2)\equiv\int_0^1 dx\frac{F_2(x,Q^2)}{x}\ . \tag{8.2}$$

Equation (8.1) then reads $I_{-1}(Q^2\rightarrow\infty)=I_{-1}=1$. In Fig. 12 we present $I_{-1}(Q^2)$ as a function of $Q^2$. The dashed line corresponds to the PWIA calculation, described in Sec. IV, in which case the effects of the FSI are neglected. The full line corresponds to the exact calculation using distorted waves, as described in Sec. VI, where the effects of the FSI are fully taken into account. The surprising result is that, for the PWIA calculation, $I_{-1}(Q^2)$ is extremely close to its asymptotic "sum rule" value for all $Q^2$ under consideration. The exact $I_{-1}(Q^2)$, however, approaches its asymptotic value at about $Q^2\approx1$ GeV$^2$. We see that the approach to scaling for $I_{-1}(Q^2)$ is completely governed by correlations,[29] which arise through the FSI between the struck and the spectator nucleon and which are neglected in the PWIA. Inspection of Fig. 12, and a detailed comparison of $F_2(Q^2,x)$ in the PWIA and in the full calculation, respectively, show that the modifications due to the FSI for the structure function $F_2$ vanish at a momentum transfer of about $Q^2\approx1$ GeV$^2$. [It was shown in Sec. VI that for our model the FSI corrections do not contribute to $F_1(Q^2,x)$.] This might suggest that the effects due to the FSI could be completely neglected for the analysis of quasielastic electron-deuteron scattering experiments for $Q^2>1$ GeV$^2$. Such a result, however, pertains only in the consideration of sum rules and different conclusions are drawn when we study $y$ scaling, for example.

We now turn to a consideration of $y$ scaling. As already pointed out in Sec. VII, quasielastic electron-deuteron scattering can be described more appropriately in terms of the scaling variable $y$ and the response func-

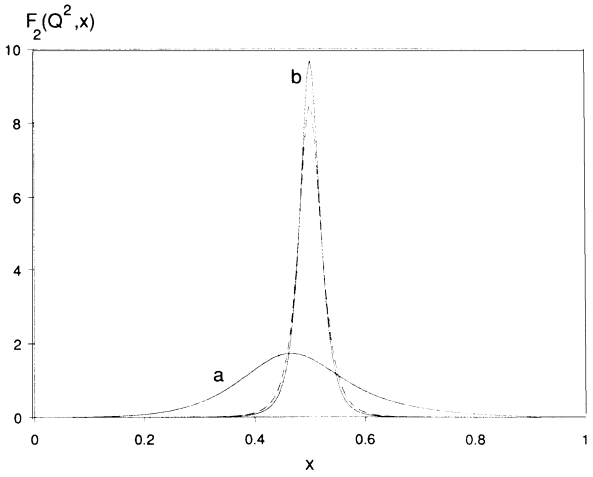


FIG. 11. The structure function $F_2(Q^2,x)$ is depicted as function of the Bjorken variable $x$ for fixed values of $Q^2$. The full line labeled $a$ represents the result for $Q^2=0.1$ GeV$^2$, the dotted line represents $Q^2=1$ GeV$^2$, the dashed line is for $Q^2=10$ GeV$^2$, and the full line labeled $b$ corresponds to $Q^2=100$ GeV$^2$, where $F_2(Q^2,x)$ has already reached its scaling value, $F_2(x)$.

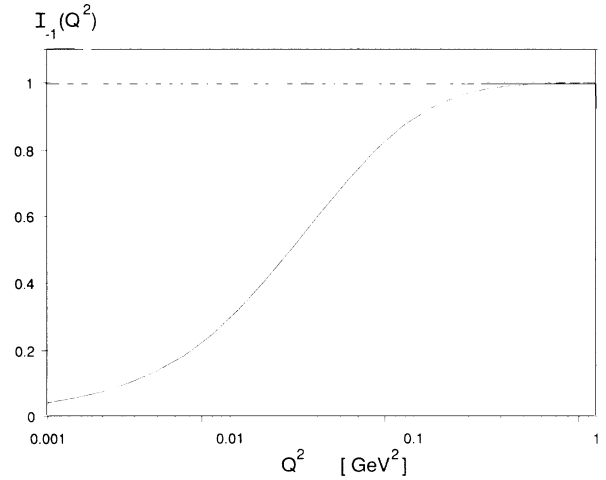


FIG. 12. The quantity $I_{-1}(Q^2)$, defined in Eq. (8.2), is shown as a function of $Q^2$. The dashed line represents the result of the PWIA calculation and the full line represents the exact calculation where the effects due to the FSI are taken into account.

tion, $F(Q^2,y)$, than in terms of $x$ and $F_{1,2}(Q^2,x)$. In the following we will therefore present our results in this notation. Note that $y$ is given by

$$y=\frac{1}{2}\left[(M+\omega)\left[1-\frac{4m^2}{s}\right]^{1/2}-|\mathbf{q}|\right] \tag{8.3}$$

[see Eq. (7.6)], and $F(Q^2,y)$ is given by

$$F(Q^2,y)=\frac{1}{m}\left[\frac{|\mathbf{q}|}{\omega}F_2(Q^2,x)+\frac{2|\mathbf{q}|}{M}F_1(Q^2,x)\tan^2\left[\frac{\theta}{2}\right]\right] \tag{8.4}$$

[see Eq. (7.9)]. From Eq. (8.4) we see that, because of the second term on the right-hand side, the relation between $F_1(Q^2,x)$ and $F_2(Q^2,x)$ and the quantity $F(Q^2,y)$ explicitly depends on the scattering angle $\theta$. The calculation shows, however, that $2|\mathbf{q}|F_1/M$ is always less than one percent of $|\mathbf{q}|F_2/\omega$ and for forward scattering we can, therefore, neglect the second term in Eq. (8.4). As previously pointed out by Butler[5] and Sick,[2] this is equivalent to assuming that the convection current contribution to the transverse part of the cross section is small compared to the magnetization current contribution, because only then is the cross section proportional to a single response function. In this approximation Eq. (8.4) thus reduces to

$$F(Q^2,y)=\frac{1}{m}\frac{|\mathbf{q}|}{\omega}F_2(Q^2,x)\ . \tag{8.4a}$$

Figure 13(a) shows the response function, $F(Q^2,y)$, calculated in the PWIA, vs $y$, for different values of the four-momentum transfer $Q^2$. Figure 13(b) shows the exact $F(Q^2,y)$, where now, and in contrast to Fig. 13(a), the effects due to the FSI are taken into account. Finally, Figs. 14(a)–14(e) show $F(Q^2,y)$ as a function of the momentum transfer $Q^2$ for six different $y$ values between 0 and $-1$ GeV. The dashed line corresponds to the PWIA calculation and the full line corresponds to the exact calculation. This way of presenting the results is called a $y$-scaling plot[8] and shows most clearly the effects due to the FSI.

One observes that, in general, the FSI corrections vanish with increasing $Q^2$, as was already pointed out in Sec. VI. We also see that at the quasielastic peak (QEP), i.e., for $y=0$, the contributions from the FSI are very small. Furthermore, it can be seen from Fig. 14(a) that, *at the* QEP, $F(Q^2,y)$ indeed exhibits remarkable scaling behavior. This is in correspondence with an analysis of the experimental data made in Ref. 8. However, the regions away from the QEP are of major physical interest, because, by means of Eq. (7.3), they may be related to the high-momentum components of nuclear wave functions. Such components, in principle, contain valuable information about the short-range behavior of nuclear interactions and of correlations,[9] and are difficult to measure in other reactions.[7] In this regime, away from the QEP, the full calculation approaches scaling from *above* with increasing $Q^2$, as do the data,[8] while the PWIA response function increases for fixed $y$ as the momentum transfer grows. This result is in full agreement with other calculations,[5,8,10] made previously.

Furthermore, Fig. 14 shows that as we consider greater (negative) values of $y$, scaling deteriorates progressively and the importance of the FSI grows. Large negative $y$ corresponds to $x$ near 1. At $x=1$, elastic scattering from the deuteron is the only allowed process and hence the FSI becomes extremely important in this region and results in large scaling violations in $F(Q^2,y)$, even for large $Q^2$, as was pointed out in Ref. 4. Therefore, we can conclude that for large negative $y$ values, the FSI are still significant at the experimental kinematics ($Q^2<10$ GeV$^2$) and our response function, $F(Q^2,y)$, does not yet scale.

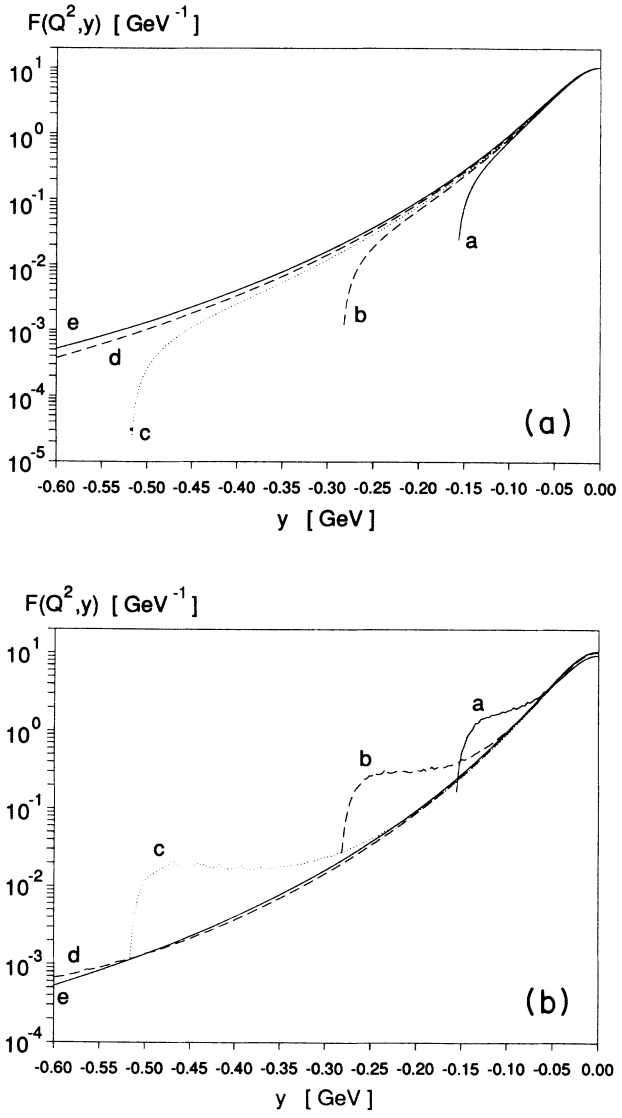


FIG. 13. The response function $F(Q^2,y)$ [see Eq. (8.4a)] is shown versus the scaling variable $y$, defined in Eq. (8.3), for different $Q^2$. In (a) the effects due to the FSI were neglected (PWIA) and in (b) those effects were fully taken into account. The labels refer to different values for $Q^2$, the square of the four-momentum transfer: *a*, $Q^2=0.1$ GeV$^2$; *b*, $Q^2=0.3$ GeV$^2$; *c*, $Q^2=1.0$ GeV$^2$; *d*, $Q^2=3.2$ GeV$^2$; *e*, $Q^2=10.0$ GeV$^2$.

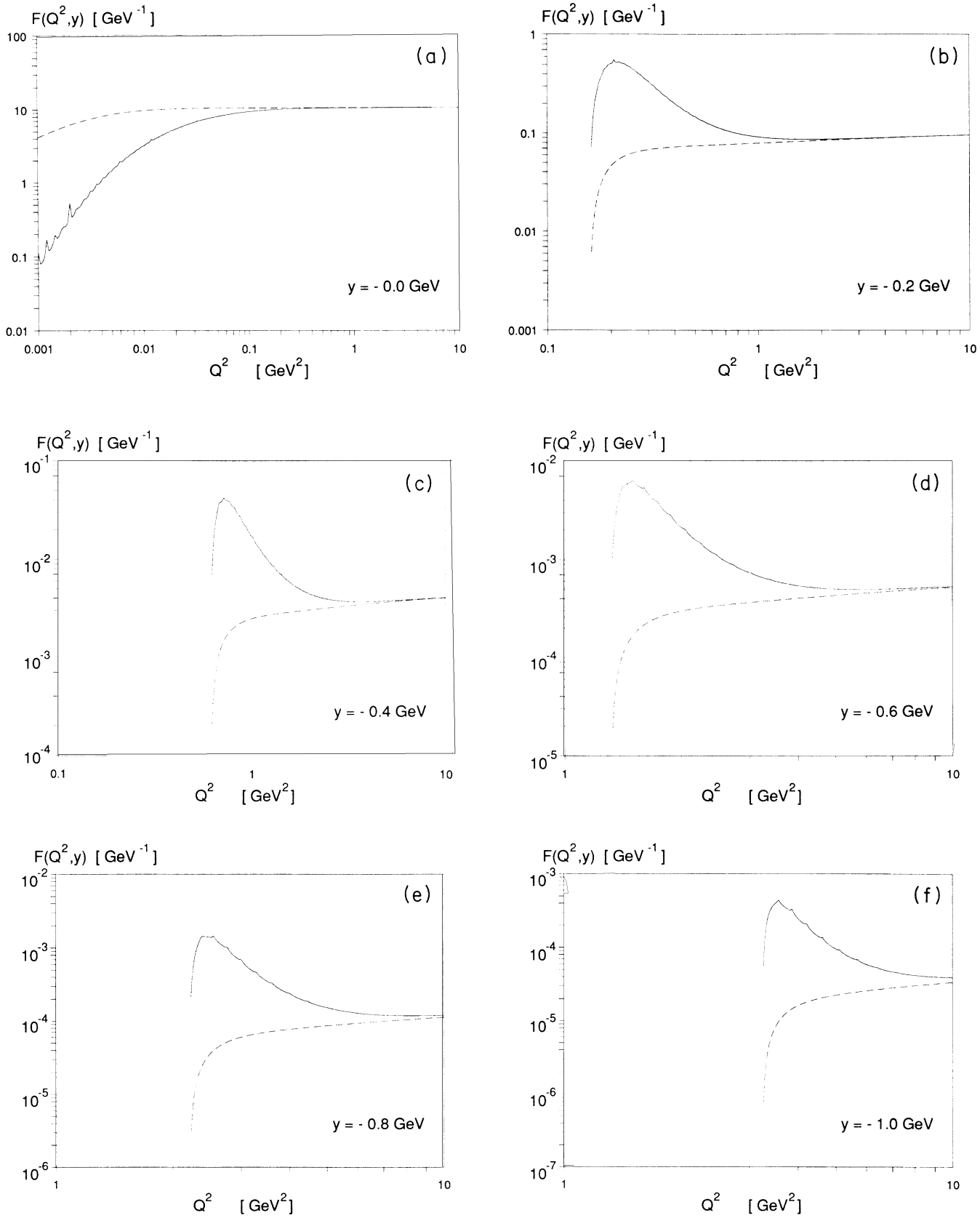


FIG. 14. $y$ scaling plot: $F(Q^2,y)$ vs $Q^2$ for fixed values of the scaling variable $y$. The dashed lines show the results of the PWIA calculations where the effects due to the FSI between the struck and the spectator nucleon were neglected. The full lines represent the exact calculations where the final state interactions were taken into account. The values of the $y$-scaling variable are (a) $y=0$ GeV, (b) $y=-0.2$ GeV, (c) $y=-0.4$ GeV, (d) $y=-0.6$ GeV, (e) $y=-0.8$ GeV, (f) $y=-1.0$ GeV.

This makes it difficult to determine the nucleon momentum distribution in the nucleus in a model-independent way, which was the final goal of those $y$-scaling experiments which have been performed.

For moderate negative values of $y$, say $|y|<0.4$ GeV, the FSI corrections become small for $Q^2>5$ GeV$^2$. However, the response function, $F(Q^2,y)$, does not scale up to the highest $Q^2$, as can be seen from Fig. 14. This again shows that the common procedure of using quasielastic scattering experiments to determine the nuclear momentum distribution is questionable unless one is able to extrapolate the experimental data to large values of $Q^2$ where FSI are less important. Finally, we note that Ji and McKeown suggest, in a recent publication,[10] that the FSI may cause the experimental response function to scale at a smaller $Q^2$ than the PWIA calculation would predict. This effect of precocious scaling cannot be confirmed by our investigation.

## IX. DISCUSSION AND CONCLUSIONS

In this work we have studied a simple model of two scalar particles interacting by means of a covariant separable interaction. The simplicity of the model allows for a comprehensive study of the electromagnetic response. The use of a covariant formalism means that we automatically include relativistic *kinematics* in our calculations and leads to an attractive formalism. However, we do not claim that we have constructed a satisfactory theory of the *dynamical* relativistic aspects of the bound state or of the scattering problem. While we have calculated the electromagnetic response up to quite large values of the momentum transfer, it is clear that nuclear physics applications are limited to the lower values of $Q^2$, where nucleons rather than quarks are the appropriate degrees of freedom.

Various useful observations may be made on the basis of our analysis. First we see that, in this model, our ability to obtain sum rules is related to the essentially nonrelativistic nature of the "deuteron" bound state. It is interesting to see that the "pole approximation" is extremely accurate for the evaluation of the electromagnetic form factor and that the accuracy of that approximation leads to a "Coulomb sum rule" that is very precisely reproduced in the plane wave impulse approximation. We have also seen how final state interactions lead to the observation that the sum rule is only reproduced for large $Q^2$, where the final state interaction may be neglected (see Fig. 12). It is also of interest to extend our study of final state interactions to targets of larger mass number, so that we may understand how such interactions would affect attempts to measure the Coulomb sum rule in inclusive $(e,e')$ reactions on nuclei.

Another topic, which has received a good deal of attention recently, is that of $y$ scaling. Our studies confirm some of the observations made by other authors: We have seen that, in the PWIA, $y$ scaling is approached from below as $Q^2$ is increased [see Fig. 13(a)], while the approach is from above if final state interactions are included [see Fig. 13(b) and Fig. 14]. Scaling behavior is well reproduced at the quasielastic peak; however, there are significant corrections due to final state interactions at large negative values of $y$. Again, it is of interest to extend these studies to larger nuclei, where one hopes to extract the momentum distribution of the nucleons in $y$-scaling studies.

In summary, we may say that, while great effort has been expended in studying nuclear properties in various inclusive and exclusive electron scattering reactions, the theoretical interpretation of the data has been somewhat limited by the belief that simple forms of the impulse approximation may be used to interpret the data obtained. One reason that such simple approximations have been used is that, to a first approximation, the mean-field approximation appears to give satisfactory results. However, difficulties in the interpretation of the longitudinal response in $(e,e')$ reactions have led various authors to question our understanding of nuclear structure within the context of the mean-field approximation.[31] For example, correlations in the target may lead to a shift of strength to higher energies and final state interactions may play some role in modifying our interpretation of the experimental data. These issues have not been resolved and require further study. In a future work we hope to extend our studies to larger systems in an attempt to understand how configuration mixing in the target and final state interactions of the struck nucleon modify our interpretation of the electromagnetic response of nuclei. In a future publication we will also discuss the momentum distribution $n(p)$ which can be derived from the response function $F(y)$ [see Eq. (7.3)]. This will involve a discussion of the nonrelativistic limit of our calculations.

## ACKNOWLEDGMENTS

This work was supported in part by the National Science Foundation, by the Faculty Research Award Program of the City University of New York, and by the Bundesministerium fuer Forschung and Technologie of the Federal Republic of Germany.

## APPENDIX A: GAUGE INVARIANCE OF THE DEUTERON CURRENT

In general, it is not trivial to show that the e.m. current is conserved. However, the demonstration of gauge invariance is simple for our separable model. We start from Fig. 2, where we replace the integration variable $k$ by $P-k$. If we further call the final deuteron momentum $P+q=P'$, we obtain the e.m. current matrix element, $F_\mu(x,Q^2)$, in analogy with Eq. (3.1):

$$F_\mu = i\int \frac{d^4k}{(2\pi)^4}\Gamma(k;P)G(P-k)G(k) \times (P+P'-2k)_\mu G(P'-k)\Gamma(k;P') . \quad \text{(A1)}$$

We see from Eq. (A1) that $F_\mu$ is a symmetric function of $P$ and $P'$. This leads to the result

$$F_\mu = (P+P')_\mu F(P^2+P'^2,P\cdot P') . \quad \text{(A2)}$$

If we contract $F_\mu$ of Eq. (A2) with $q^\mu=(P'-P)^\mu$, we find

$$q^\mu F_\mu = (P'^2-P^2)F(P^2+P'^2,P\cdot P') . \quad \text{(A3)}$$

This is our final result. It shows that in the elastic case, i.e., if the final deuteron is on its mass shell, $P'^2=P^2=M^2$, the matrix element of the e.m. current satisfies the gauge invariance condition, $q^\mu F_\mu=0$. However, this is not true if $P'^2\neq M^2$, as can also be seen from Eq. (A3). In that case we will simply neglect the longitudinal part of $F_\mu(x,Q^2)$ and also use Eq. (3.2).

## APPENDIX B: THE CALCULATION OF THE ELASTIC ELECTROMAGNETIC FORM FACTOR

If we carry out our calculation in the rest frame of the deuteron, we find, upon using Eqs. (3.1) and (3.2), the elastic e.m. form factor

$$F_0(Q^2)=2i\frac{|\mathbf{q}|^2}{Q^2}\frac{N^2}{(2\pi)^3}\times\int_0^\infty d|\mathbf{k}||\mathbf{k}|^2 g(|\mathbf{k}|^2)\times\int_{-1}^{1} d\cos\theta I(|\mathbf{k}|,\cos\theta)\ . \tag{B1a}$$

Here

$$I(|\mathbf{k}|,\cos\theta)=\int_{-\infty}^{\infty} dk_0 g(k_c^2)\frac{k_0-\omega|\mathbf{k}|\cos\theta/|\mathbf{q}|}{(k_0-z_1)\cdots(k_0-z_6)}\ . \tag{B1b}$$

$N$ is the norm which is fixed by the condition $F_0(Q^2=0)=1$, and $g(|\mathbf{k}|^2)$ and $g(k_c^2)$ are the covariant form factors, defined in Eq. (2.9), with

$$k_c^2=|\mathbf{k}|^2[1-(\cos\theta)^2]+\frac{|\mathbf{q}|^2}{M^2}\left[k_0-M-\frac{M+\omega}{|\mathbf{q}|}|\mathbf{k}|\cos\theta\right]^2\ , \tag{B2}$$

For the elastic process, $F_0$ is a function of $Q^2$ only, because then $\omega$ and $|\mathbf{q}|$ are fixed by means of the relation $x=Q^2/(2M\omega)=1$.

The term $(k_c^2+m^2)^{1/4}$ in $g(k_c^2)$ [see Eq. (2.9)] leads to two branch cuts in the complex $k_0$ plane, one in the upper and one in the lower half plane. The term $1/(k_c^2+\Lambda^2)$ in $g(k_c^2)$ is responsible for two singularities of the integrand of $I(|\mathbf{k}|,\cos\theta)$ where, once again, one is in the upper and one is in the lower half plane. Thus, no matter how we perform the contour integration in the evaluation of $I(|\mathbf{k}|,\cos\theta)$, the presence of $g(k_c^2)$ always contributes one branch cut and one pole.

However, by far the most important contributions to $I(|\mathbf{k}|,\cos\theta)$ arise from the poles, $z_1$ to $z_6$, of the propagators $G(k)$, $G(P-k)$, and $G(k+q)$. We find

$$z_1=E(\mathbf{k})-i\varepsilon\ , \tag{B3a}$$

$$z_2=-E(\mathbf{k})+i\varepsilon\ , \tag{B3b}$$

$$z_3=M-E(\mathbf{k})+i\varepsilon\ , \tag{B3c}$$

$$z_4=M+E(\mathbf{k})-i\varepsilon\ , \tag{B3d}$$

$$z_5=-\omega+E(\mathbf{k}+\mathbf{q})-i\varepsilon\ , \tag{B3e}$$

$$z_6=-\omega-E(\mathbf{k}+\mathbf{q})+i\varepsilon\ , \tag{B3f}$$

where $E(\mathbf{k})=(|\mathbf{k}|^2+m^2)^{1/2}$ and $E(\mathbf{k}+\mathbf{q})=(|\mathbf{k}+\mathbf{q}|^2+m^2)^{1/2}$. $z_1$, $z_3$, and $z_5$ are the positive energy (particle) poles of the propagators $G(k)$, $G(P-k)$, and $G(k+q)$, and $z_2$, $z_4$, and $z_6$ are the corresponding negative energy (antiparticle) poles.

Due to the highly nonrelativistic character of the "deuteron" bound state, i.e., the very weak binding, the nucleons are close to being on-mass-shell and propagate mostly as free *particles*. Their propagation as *antiparticles* is highly suppressed and, thus, the antiparticle poles of the propagators, $z_2$, $z_4$, and $z_6$, contribute only a negligible portion to the integral $I(|\mathbf{k}|,\cos\theta)$ of Eq. (B1b). This means that, if we close the path for the contour integration in the upper half plane, our result will be completely dominated by the residue of the pole at $z_3$, and, if we close the path in the lower half plane, it will be dominated by the sum of the residues of the poles at $z_1$ and $z_5$.

In the "pole approximation," we replace the free propagator $G(P-k)$ by its corresponding "on-shell" expression [see Eq. (3.6)]:

$$G(P-k)\to H(P-k)=-2\pi i\frac{\delta\{k_0-[M-E(\mathbf{k})]\}}{2E(\mathbf{k})}\ . \tag{B4}$$

If we evaluate $I(|\mathbf{k}|,\cos\theta)$ of Eq. (B1b) by contour integration in the upper half plane, it is a sum of five terms: the branch cut and the pole contribution arising from $g(k_c^2)$, the contributions from the antiparticle poles of $G(k)$ and $G(k+q)$, $z_2$ and $z_6$, and the contribution of the particle pole of $G(P-k)$ at $z_3$. Applying the "pole approximation" of Eq. (B4) is equivalent to dropping the first four terms in this sum. That this is an excellent approximation can be seen from Fig. 4, where we compare the full calculation with this approximation. Especially for small $Q^2$, the deviation between both calculations is about 1 part in $10^4$ and thus far below the accuracy of our numerical computations. Again, the reason for this excellent agreement is the highly nonrelativistic character of the "deuteron" bound state, i.e., the fact that due to the weak binding the nucleons propagate almost exclusively as free *particles*, with the admixture of *antiparticle* components to the "deuteron" wave function being quite small.

[1]G. B. West, Phys. Rep. **18C**, 264 (1975).
[2]I. Sick, D. Day, and J. S. McCarthy, Phys. Rev. Lett. **45**, 871 (1980).
[3]M. N. Butler and R. D. McKeown, Phys. Lett. B **208**, 171 (1988).
[4]G. Yen, H. Harindranath, J. P. Vary, and H. J. Pirner, Phys. Lett. B **218**, 408 (1989).
[5]M. N. Butler and S. E. Koonin, Phys. Lett. B **205**, 123 (1988).
[6]S. A. Gurvitz and A. S. Rinat, Phys. Rev. C **35**, 696 (1987).
[7]I. Sick, Phys. Lett. **157B**, 13 (1985).
[8]C. d. Atti, E. Pace, and G. Salme, Phys. Rev. C **36**, 1208 (1987).
[9]X. Ji and J. Engel, Phys. Rev. C **40**, R497 (1989).

[10]X. Ji and R. D. McKeown, California Institute of Technology report, 1990.
[11]G. Rupp and J. A. Tjon, Phys. Rev. C **37**, 1729 (1988).
[12]M. J. Zuilof and J. A. Tjon, Phys. Rev. C **22**, 2369 (1980).
[13]G. Rupp, L. Streit, and J. A. Tjon, Phys. Rev. C **31**, 2285 (1985).
[14]E. Salpeter and H. Bethe, Phys. Rev. **84**, 1232 (1951).
[15]Some discussion of the Bethe-Salpeter equation and its use in nuclear physics may be found in L. S. Celenza and C. M. Shakin, *Relativistic Nuclear Physics* (World Scientific, Singapore, 1986).
[16]V. M. Bannur, L. S. Celenza, H. Chen, S. Gao, and C. M. Shakin, Int. J. Mod. Phys. A **5**, 1479 (1990).
[17]M. Lacombe, B. Loiseau, J. M. Richard, R. Vinh Mau, J. Cote, P. Pires, and R. d. Tourreil, Phys. Rev. C **21**, 861 (1980).
[18]R. W. Berard, F. R. Buskirk, E. B. Dally, J. N. Dyer, X. K. Maruyama, R. L. Topping, and T. J. Traverso, Phys. Lett. **47B**, 355 (1973).
[19]J. D. Bjorken, Phys. Rev. **148**, 1467 (1966).
[20]F. E. Close, *Introduction to Quarks and Partons* (Academic, New York, 1979).
[21]N. F. Mott, Proc. R. Soc. London, Ser. A **124**, 425 (1929).
[22]E. Leader and E. Predazzi, *Gauge Theories and New Physics* (Cambridge University, Cambridge, 1982).
[23]T. Muta, *Foundations of Quantum Chromodynamics* (World Scientific, Singapore, 1987).
[24]J. D. Bjorken, Phys. Rev. **179**, 1547 (1969).
[25]C. Callan and D. Gross, Phys. Rev. Lett. **22**, 156 (1969).
[26]L. S. Celenza, Phys. Rev. C **19**, 447 (1979).
[27]D. J. Ernst, C. M. Shakin, and R. M. Thaler, Phys. Rev. C **8**, 46 (1973).
[28]R. Rosenfelder, Ann. Phys. (N.Y.) **128**, 188 (1980).
[29]G. B. West, Lectures given at the International Summer School on Nuclear Dynamics, Dronten, The Netherlands, August 1988 (unpublished).
[30]E. J. Moniz, I. Sick, R. R. Whitney, R. J. Ficenec, R. D. Kephart, and W. P. Trower, Phys. Rev. Lett. **26**, 445 (1971).
[31]For a recent review, see S. Drozdz, S. Nishizaki, J. Speth, and J. Wambach, Kernforschungsanlage Juelich Report No. P/90/3/42, 1990.